Savage, R. O. Burford, W. T. Kinoshita, *ibid.*, p. 175].
6. R. S. Yeats, *J. Geophys. Res.* **88**, 569 (1983); *Science* **196**, 295 (1979).
7. K. Satake and K. Abe [*J. Phys. Earth* **31**, 217 (1983) examine the Niigata earthquake and its aftershocks.
8. A. Cisternas [*Bull. Seismol. Soc. Am.* **53**, 1075 (1963)] examined the Kern County earthquake. M. Ouyed, G. Yielding, D. Hatzfield, and G. C. P. King [*Geophys. J. R. Astron. Soc.* **73**, 605 (1983)] investigated El Asnam aftershocks.
9. J. Eaton, R. Cockerham, F. Lester, in *Calif. Div. Mines Geol. Spec. Publ. 66* (1983), pp. 261–274; R. A. Uhrhammer, R. B. Darragh, B. A. Bolt, *ibid.*, pp. 221–232.
10. S. H. Hartzell and T. H. Heaton, *ibid.*, pp. 241–246; H. Kanamori, *ibid.*, pp. 233–240.
11. E. Fielding, M. Barazangi, L. Brown, J. Oliver, and S. Kaufman (*ibid.*, pp. 137–150) and C. M. Wentworth, A. W. Walter, J. A. Bartow, and M. D. Zoback (*ibid.*, pp. 113–126) interpret seismic refraction and reflection profiles beneath the Kettleman Hills anticline, 65 km south of the Coalinga main shock, as showing a steeply northeast dipping reverse fault with 0.5 to 1.0 km of displacement and a gently southwest dipping thrust fault with about 10 km of cumulative slip.
12. G. King and R. Stein, *ibid.*, pp. 165–176.
13. A. W. Burnett and S. A. Schumm [*Science* **222**, 49 (1983)] use similar techniques in the central United States.
14. Time-stratigraphic correlation of the Holocene Panoche alluvial-fan surface (Fig. 2A) from the soil survey of the Coalinga area [*U.S. Dept. Agric. Ser. 1944* (1952) and the age of the Tulare Formation are reviewed by W. R. Lettis [*U.S. Geol. Surv. Open-File Rep. 82-526* (1982)]. B. Atwater (in preparation) furnished the radiocarbon age.
15. The earthquake elevation changes are closely correlated with topography. After a regional slope of 0.37° is removed from the leveling route topography, the topographic height is equal to about 300 times the 1983 elevation change. The amplitude of the topography is damped relative to the structural contours, however, by erosion from the ridge crest and deposition into lows. The late Pleistocene beds of the Tulare Formation dip 4 to 16 times more steeply than the topographic slope of the anticline. Thus, the minimum cumulative fault slip since deposition of the beds becomes 1.8 m × 300 × 4 = 2 km.
16. T. W. Dibblee, *U.S. Geol. Surv. Open-File Rep. 71–87* (1971).
17. G. C. P. King and C. Via-Finzi, *Nature (London)* **292**, 22 (1981); G. Yielding, J. A. Jackson, G. C. P. King, H. Sinvhal, C. Vita-Finzi, R. M. Wood, *Earth Planet. Sci. Lett.* **56**, 287 (1981); Y. Thommeret, G. C. P. King, C. Vita-Finzi, *ibid.* **63**, 137 (1983).
18. H. Philip and M. Meghraoui, *Tectonics* **2**, 17 (1983).
19. J. C. Ruegg, M. Kasser, A. Tarantola, J. C. Lepine, B. Chouikrat, *Bull. Seismol. Soc. Am.* **72**, 2227 (1982).
20. R. S. Stein and W. Thatcher, *J. Geophys. Res.* **86**, 4913 (1981).
21. W. S. Dunbar, D. M. Boore, W. Thatcher, *ibid.* **70**, 1893 (1980).
22. Y. Ota [*GeoJournal* **4**, 111 (1980)] reviewed the deformed Quaternary shorelines; T. Kato [*Tectonophysics* **97**, 183 (1983)] measured the historic shoreline deformation from tide gage records.
23. H. Kawasumi, Ed., *General Report on the Niigata Earthquake of 1964* (Tokyo Electrical Engineering College Press, Tokyo, 1973); *Submarine Geological Chart of the Adjacent Seas of Nippon* (Marine Safety Agency, Tokyo, 1973).
24. Compare the distribution of released seismic energy by historic earthquakes (figure 5-13), to the distribution of faults (figure 5-14) and folds (figure 5-15), in *Explanatory Text of the Quaternary Tectonic Map of Japan* (National Research Center for Disaster Prevention, Tokyo, 1973).
25. Research Group for Quaternary Tectonic Map, *Quaternary Tectonic Map of Japan* (National Research Center for Disaster Prevention, Tokyo, 1969); Research Group for Active Faults, *Active Faults in and Around Japan* (Univ. of Tokyo Press, Tokyo, 1980).
26. We are indebted to S. Lack, G. Mavko, A. McGarr, R. Wallace, C. Wentworth, R. Yerkes, and J. Ziony for incisive reviews. This is Cambridge Earth Sciences contribution 492. The order of authorship was chosen by lot. This work was supported by the Royal Society of London and National Environment Research Council grant GR3-3904.

13 January 1984; accepted 23 February 1984

Chondrites: A Trace Fossil Indicator of Anoxia in Sediments

Abstract. *The trace fossil* Chondrites, *a highly branched burrow system of unknown endobenthic deposit feeders, occurs in all types of sediment, including those deposited under anaerobic conditions. In some cases, such as the Jurassic Posidonienschiefer Formation of Germany,* Chondrites *occurs in black, laminated, carbonaceous sediment that was deposited in chemically reducing conditions. In other cases, such as numerous oxic clastic and carbonate units throughout the geologic column,* Chondrites *typically represents the last trace fossil in a bioturbation sequence. This indicates that the burrow system was produced deep within the sediment in the anaerobic zone below the surficial oxidized zone that was characterized by freely circulating and oxidizing pore waters.*

The primary importance of trace fossils (biogenic sedimentary structures) to geologists is their great utility in reconstructing various aspects of ancient depositional environments, including paleobathymetry, hydraulic regime during sedimentation, and original character of the substrate (*1*). Chemical aspects of the original environment, including salinity, *p*H, and redox potential of interstitial and bottom waters, are not as easy to ascertain.

The trace fossil *Chondrites* may provide us with a means of determining redox conditions in the original sediment. *Chondrites* is a regularly branched burrow system constructed by endobenthic deposit-feeding animals of unknown taxonomic affinity (*2*). It is a distinctive trace fossil, characterized by a rootlike structure of branching shafts and tunnels in which the branching angle is a relatively constant 30° to 40° and the shaft or tunnel diameter, which may be 0.1 to 10 mm, is uniform throughout any single system. Virtually all descriptions of *Chondrites* in Paleozoic, Mesozoic, and Cenozoic rocks, including both terrigenous and carbonate sediment, show that the burrow was emplaced well below the water-sediment interface. The nature of its occurrence usually indicates that the burrow was kept open by its inhabitant and was later filled passively with sediment from above.

Chondrites is common in a wide variety of sedimentary rocks deposited over the past half billion years (*2, 3*). The burrows are still being produced in marine sediments today, but all known modern occurrences are in deep-sea deposits (*4*). Although no living or dead animal actually has been discovered inside a *Chondrites* burrow, let alone in the process of constructing a *Chondrites*, Swinbanks and Shirayama (*5*) have circumstantial evidence suggesting the burrower to be an infaunal abyssal nematode. In general, errant marine nematodes are organic detritus-feeders, many of which construct open burrows.

Chondrites is easily recognized in sedimentary rocks but is notorious among geologists as a facies-breaking trace—that is, it defies generalization as an exclusive feature of any particular sedimentary facies. Although it is not omnipresent, it may be found in a wide variety of rock types (sandstone, shale, and limestone) representing deposition in a broad spectrum of marine environments (from subtidal shelves to the abyssal realm).

We suggest that *Chondrites* is made in anaerobic sediment, commonly beneath oxygen-starved sea floors; thus that the presence of *Chondrites* in a deposit indicates very low oxygen levels in the interstitial waters within the sediment at the site of burrow emplacement. Oxygen-poor conditions influence the distribution of *Chondrites*-making organisms to a much more significant degree than do bathymetry or sediment type.

Black, laminated, carbonaceous clay generally can be considered an anoxic sediment, deposited where interstitial waters contained insufficient oxygen to oxidize volatile organic compounds in the sediment. Some such laminated clays contain burrows, indicating that in those cases bottom conditions were not totally inhospitable to infaunal life, but commonly only one burrow type is present. Almost invariably it is *Chondrites*. The Lower Jurassic (Toarcian) Posidonienschiefer Formation in southern Germany exemplifies this type of occurrence (*6*), where at certain horizons *Chondrites* occurs profusely and to the near exclusion of all other trace fossils in a black, carbonaceous shale (Fig. 1A) that also contains exquisitely preserved body fossils with very delicate features (crinoids) and even organic tissues (marine reptiles and fish; the periostracum of ammonites).

Trace fossil assemblages in Lower Cretaceous (Barremian-Albian) deep-sea deposits from the Atlantic Ocean reflect the response of benthic communities to major changes in oxygen concentrations of bottom and interstitial waters during cyclic oceanic anoxic events (*7, 8*). Light-colored, totally bioturbated limestone containing a diverse trace fossil suite alternates regularly with black,

laminated mudstone. *Chondrites* occurs, typically to the exclusion of all other trace fossils, in layers immediately overlying and underlying the dark-colored, organic-rich, unburrowed mudstone. Assuming that the mudstone represents a period of total anoxia at the sea floor, *Chondrites* reflects an environmental tolerance of oxygen levels lower than any other ichnogenus.

In the Upper Cretaceous (Cenomanian) Plenus Marls of northern Germany, dense concentrations of *Chondrites* occur in a laminated, gray stratum so obvious and exceptional that it can be used as a facies-crossing chronostratigraphic marker based on the presence of this one trace fossil (Fig. 1B). *Chondrites* specimens are small and accompanied by only a few very small, poorly developed specimens of *Zoophycos*, which they postdate. Since bioturbation is incomplete, anoxia is to be suspected. The Plenus Marls represent one of the major oceanic anoxic events that affected the oceans worldwide (*8*).

In the Upper Cretaceous (Coniacian-Santonian) Austin Chalk of Texas, *Chondrites* is a common trace fossil in both bioturbated sequences and dark-colored, laminated units (Fig. 1C). The depth of emplacement of *Chondrites* in the sediment varies considerably. In intensely bioturbated chalk, that depth may have been several decimeters below the water-sediment interface; but in laminated zones, where *Chondrites* occurs to the exclusion of most other trace fossils, it is doubtful that the small *Chondrites* branches extended more than 3 to 5 cm below the sediment surface.

Totally bioturbated white chalk units of Upper Cretaceous (Cenomanian-Maastrichtian) age in northern Europe contain abundant *Chondrites* (*9*). Crosscutting relations of various trace fossils in the chalk indicate that small *Chondrites* almost always is the last trace to be produced in the bioturbation sequence. In many cases, *Chondrites* in the chalk is restricted more or less to the fill of other burrows, especially *Thalassinoides*. Assuming continuous chalk sedimentation without erosion, *Chondrites* must have been emplaced at a greater depth in the sediment than any other associated trace fossil (*10*). This is very surprising, because *Chondrites* usually is also the smallest trace fossil in the assemblage; and in situations where several different sizes of *Chondrites* cooccur, the smallest is always the last in the burrowing sequence (Fig. 1D). The order of burrow emplacement represents tiering of the endofauna within the sediment, and the fact that the apparently smallest organisms reached deepest shows that the limiting factor was not one of size of burrower or burrow. Rather it would appear to be tolerance to low oxygen levels; small organisms generally are recognized as having greater tolerance of anoxia than larger ones (*11*).

In low-diversity trace fossil associations; in chalks at least, it is commonly the upper tiers of burrows that are the first to disappear, followed by midlevel tiers, until *Chondrites* remains alone or as the heavily dominant form (Fig. 2). This sequence invites an interpretation based on oxygen levels of the bottom waters. We suggest that *Chondrites* is made by organisms having particularly great tolerance of low oxygen levels, penetrating further below the redox boundary in the sediment than other endofauna in well-oxygenated situations (perhaps at depths of 1 m or more in chalk ooze), and colonizing sea floors where the bottom water is insufficiently oxygenated for other endobenthos.

Chondrites occur in Mesozoic and Cenozoic deep-sea pelagic deposits of all lithologies, as seen in worldwide Deep-Sea Drilling Project cores. Here too, *Chondrites* represents the latest and therefore deepest of all the ichnogenera in the deep-sea trace fossil association to be emplaced in the sediment (*12*). Thus, even in the abyssal environment, *Chondrites* apparently is produced in an oxygen-depleted zone that lies beneath the

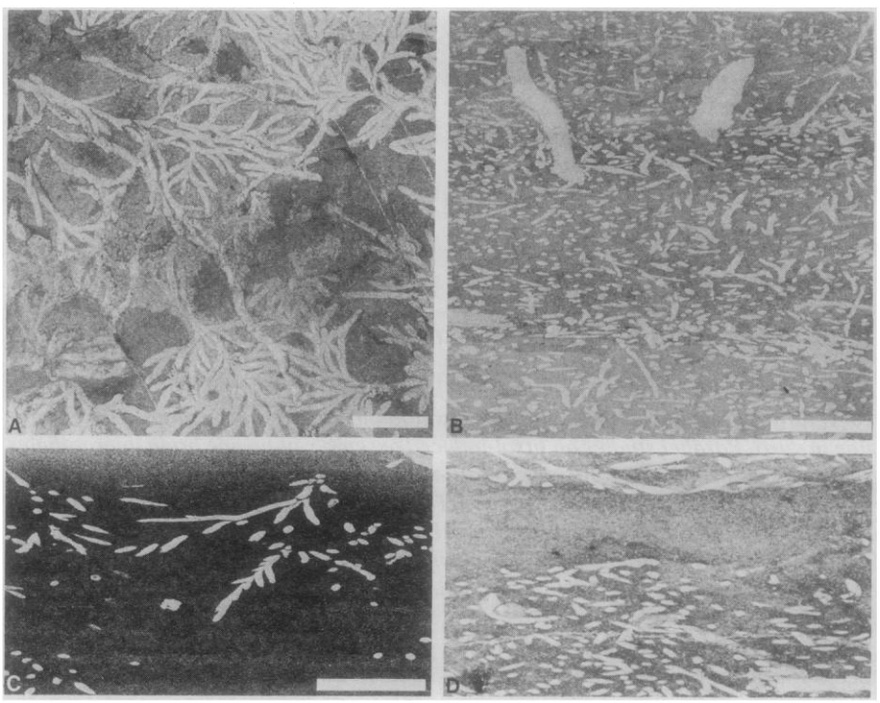

Fig. 1. Densely packed *Chondrites* in a variety of lithologies. (A) Black, laminated shale of the Posidonienschiefer, Jurassic (Toarcian), Holzmaden, Germany (scale bar, 1 cm). (B) Dark gray marl of the Plenus Marls, Cretaceous (Cenomanian), Hannover, Germany (scale bar, 1 cm). (C) Brick-red marl of the Austin Chalk, Cretaceous (Coniacian-Santonian), Dallas, Texas (scale bar, 1 cm). (D) Marly chalk, Cretaceous (Maastrichtian), Jylland, Denmark (scale bar, 0.5 cm).

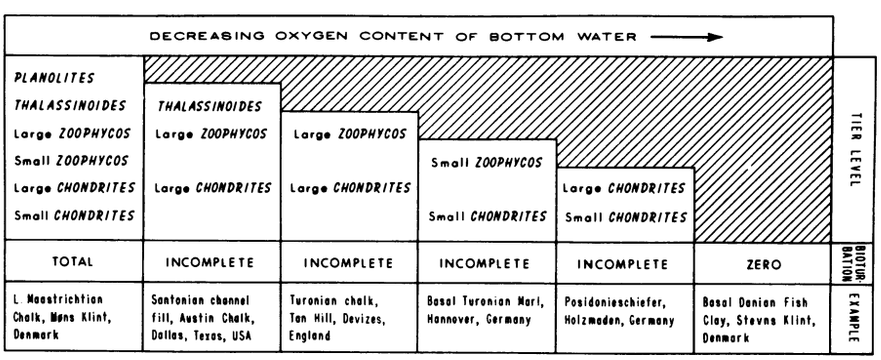

Fig. 2. Tiering relations of trace fossils, primarily oxygen-controlled, in selected examples of Mesozoic marine strata that represent oxic to anoxic depositional environments.

oxidized surficial layer of the fine-grained ooze.

Chondrites is a facies breaker because it occurs in situations where there is a gradual redox boundary within burrowing reach of the sea floor and in sediment that is rich in organic (nutritious) material; this situation underlies many sorts of sea floors. The burrow has a distinctive and elaborate morphology; it does not reflect the sort of generalized pattern that might be expected in a trace-making animal with broad environmental tolerances. The occurrence of *Chondrites* is related to chemically reducing conditions deep within the sediment and is only indirectly dependent on sea-floor conditions.

RICHARD G. BROMLEY
Institute of Historical Geology and Palaeontology, 1350 Copenhagen K, Denmark
A. A. EKDALE
Department of Geology and Geophysics, University of Utah, Salt Lake City 84112

References and Notes

1. A. Seilacher, in *Approaches to Paleoecology* (Wiley, New York, 1964), pp. 296–316; *Mar. Geol.* **5**, 413 (1967); J. D. Howard, in *The Study of Trace Fossils* (Springer, New York, 1975), pp. 131–146; D. C. Rhoads, in *ibid.* pp. 147–160.
2. S. Simpson, *Q. J. Geol. Soc. London* **112**, 475 (1957); A. Seilacher and D. Meischner, *Geol. Rundsch.* **54**, 596 (1964); R. G. Osgood, *Palaeontogr. Am.* **6**, 281 (1970); M. L. Shourd and H. L. Levin, *J. Paleontol.* **50**, 260 (1976).
3. W. Häntzschel, in *Treatise on Invertebrate Paleontology* (Univ. of Kansas Press, Lawrence, 1975), part W, Suppl. 1, pp. 1–269.
4. A. A. Ekdale and W. H. Berger, *Palaeogeogr. Palaeoclimatol. Palaeoecol.* **23**, 263 (1978); A. Wetzel, *Meteor Forschungsergeb. Ergeb.* **34**, 1 (1981).
5. D. D. Swinbanks and Y. Shirayama, in preparation.
6. K. Brenner and A. Seilacher, *Neues Jahrb. Geol. Palaeontol. Abh.* **157**, 11 (1978); E. G. Kauffman, *ibid.*, p. 18.
7. A. A. Ekdale, *Soc. Econ. Paleontol. Mineral. Spec. Pub. 35*, (1984).
8. M. A. Arthur and S. O. Schlanger, *Am. Assoc. Petrol. Geol. Bull.* **63**, 870 (1979).
9. R. G. Bromley, *Geol. Soc. London Q. J.* **123**, 157 (1967); W. J. Kennedy, *Br. Mus. Nat. Hist. Geol. Bull.* **15**, 127 (1967).
10. A. A. Ekdale and R. G. Bromley, *Bull. Geol. Soc. Den.* **31**, 107 (1983).
11. D. Rhoads and J. Morse, *Lethaia* **4**, 413 (1971).
12. A. A. Ekdale, *Geol. J.* (special issue) **9**, 163 (1977).
13. We thank J. Aagaard for photographic assistance. Supported in part by NSF grant EAR 8305869 to A.A.E.

26 January 1984; accepted 20 March 1984

Inhibition of Plant Microtubule Polymerization in vitro by the Phosphoric Amide Herbicide Amiprophos-Methyl

Abstract. *The phosphoric amide herbicide amiprophos-methyl (APM) produced a concentration-dependent inhibition of taxol-induced rose microtubule polymerization in vitro. Parallel studies on taxol-induced assembly of bovine brain microtubules showed no effect of APM at a concentration ten times that required to give complete inhibition of rose microtubule assembly. The data indicate that (i) APM is a specific and potent antimicrotubule drug and (ii) APM directly poisons microtubule dynamics in plant cells, rather than indirectly depolymerizing microtubules through a previously proposed mechanism involving deregulation of intracellular calcium levels.*

The phosphoric amide herbicides have been considered antimicrotubule drugs on the basis of the observed disappearance of microtubules (*1*) and the disruption of microtubule-dependent processes (*2*) in vivo after the drugs are applied to cells of either higher or lower plants. That these drugs interact directly with the microtubule system in plant cells has not been shown. In fact, the best characterized member of this class of herbicides, amiprophos-methyl (APM), affects cellular processes other than the microtubule system. For example, APM at concentrations greater than 5 μ*M* inhibits the uptake of $^{45}Ca^{2+}$ by mitochondria and microsomes isolated from corn and squash (*3*), and at 10 μ*M* inhibits $^{45}Ca^{2+}$ uptake, photosynthesis, and respiration in the unicellular alga *Chlamydomonas* (*4*). However, APM does not inhibit the assembly of mammalian brain microtubules in vitro, depolymerize preformed brain microtubules, or prevent the initiation of brain microtubule assembly on algal microtubule organizing centers in vitro (*1*). These observations, along with the knowledge that brain microtubules are depolymerized in vitro by calcium and that microtubules in animal cells depolymerize after ionophore-mediated calcium influx (*5*), have led to the proposal that APM acts only indirectly on microtubules in plant cells by deregulation of cellular calcium stores with subsequent microtubule depolymerization (*3*, *4*, *6*).

To determine whether APM interferes directly with plant microtubule assembly, we examined the effects of this herbicide on the polymerization of plant tubulin into microtubules in vitro. We showed earlier (*7–9*) that tubulin isolated from cultured cells of rose (*Rosa* sp.) assembles into microtubules after being warmed in the presence of either glycerol or taxol (*10*). Because the taxol-mediated assembly of rose tubulin was so efficient and easily controlled (*7*, *9*) we used this system in the present study of APM.

Rose tubulin was isolated by DEAE–Sephadex A50 chromatography as described (*7*), with minor modifications (*8*), and was more than 85 percent pure as judged by quantitative densitometry of Coomassie blue–stained sodium dodecyl sulfate slab gels (*9*). The kinetics of taxol-mediated rose microtubule assembly at 24°C was monitored turbidimetrically by measuring absorbancy at 400 nm (*11*). Rose tubulin at 10 μ*M* (*12*) assembled rapidly in the presence of a saturating concentration of taxol (40 μ*M*) (*9*), with the kinetics showing a short lag phase followed by a rapid increase in absorbancy and maximum absorbancy reached within 1 hour (Fig. 1). Assembly of tubulin in the presence of micromolar levels of APM produced concentration-dependent increases in the lag time and decreases in both the rate and extent of turbidity development. Maximum inhibition of turbidity development was obtained at nearly 1:1 molar ratios of APM to tubulin. The kinetics of turbidity change with 10 μ*M* APM contained early negative absorbancy values followed by a small amount of recovery to produce a net change in absorbancy of zero by 25 minutes. The early decrease in absorbancy probably results from the dissociation of small aggregates of tubulin that were not sedimented during the tubulin isolation procedure (*8*, *9*). When DEAE-purified (*8*, *13*) bovine brain tubulin (10 μ*M*)

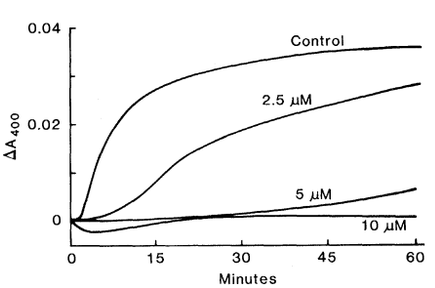

Fig. 1. Effect of APM on the kinetics of taxol-induced microtubule assembly. Samples of tubulin (10 μ*M*) in sucrose isolation buffer (SIB) (*8*) at 0°C were mixed rapidly with SIB at 24°C containing saturating taxol (40 μ*M*) and a given amount of APM (2.5, 5, or 10 μ*M*). Assembly reaction mixtures were monitored continuously at 24°C in 400-μl quartz cuvettes (light path, 1 cm) in a recording spectrophotometer (Beckman Acta III), and turbidity was recorded as the change in absorbancy at 400 nm (ΔA_{400}). All assembly mixtures contained 1.5 percent DMSO, including the control, which contained no APM.